

## Epigenetic network of EZH2/SFRP1/Wnt in the epithelial-mesenchymal transition of laryngeal carcinoma cells

Wei CHEN<sup>1,2,\*</sup>, Hua-Tao WANG<sup>3,\*</sup>, Jun-Feng JI<sup>1,2</sup>, Zhi-Yi WANG<sup>1,2</sup>, Tao SHI<sup>1,2</sup>, Ming-Hai WU<sup>1,2</sup>, Peng-Ju YU<sup>4,\*</sup>

<sup>1</sup>Department of Otolaryngology-Head and Neck Surgery, Jinling Hospital Affiliated to Nanjing University, Nanjing, Jiangsu, China; <sup>2</sup>Department of Otolaryngology-Head and Neck Surgery, The First School of Clinical Medicine Affiliated to Southern Medical University, Guangzhou, Guangdong, China; <sup>3</sup>Department of Otolaryngology-Head and Neck Surgery, Huai'an Hospital of Huai'an City, Huai'an, Jiangsu, China; <sup>4</sup>Department of Otolaryngology-Head and Neck Surgery, Kunshan Hospital of Traditional Chinese Medicine, Kunshan, Jiangsu, China

\*Correspondence: yupengju1014@163.com

#Contributed equally to this work.

Received December 8, 2021 / Accepted March 18, 2022

Enhancer of Zeste Homologue 2 (EZH2) as a histone methyltransferase epigenetically regulates laryngeal carcinoma (LGC) progression. The present study sought to explore the role and mechanism of EZH2 in the epithelial-mesenchymal transition (EMT) of LGC cells. Expressions of EZH2, secreted frizzled-related protein 1 (SFRP1), and trimethylation of lysine 27 on histone H3 (H3K27me3) in LGC tissues or cells were detected via reverse transcription quantitative polymerase chain reaction (qRT-PCR) and western blotting. Upon transfection of si-EZH2, si-SFRP1, oe-SFRP1, or H3K27me3 upregulation, cell viability was assessed via cell counting kit-8, protein levels of E-cadherin, N-cadherin,  $\beta$ -catenin, c-Myc, and Cyclin D1 were determined via western blotting, and Vimentin expression was determined via immunofluorescence. The enrichment level of H3K27me3 in the SFRP1 promoter was measured via chromatin immunoprecipitation-PCR. EZH2 was highly expressed in LGC tissues and cells. Silencing EZH2 repelled the EMT of LGC cells. Mechanically, EZH2 upregulated H3K27me3 in the SFRP1 promoter to inhibit SFRP1 expression, and SFRP1 overexpression inactivated the Wnt pathway. H3K27me3 upregulation or SFRP1 downregulation reversed the inhibition of silencing EZH2 in the EMT of LGC cells. Overall, EZH2 upregulated H3K27me3 in the SFRP1 promoter to inhibit SFRP1 expression and activate the Wnt pathway, thereby facilitating the EMT of LGC cells.

*Key words: laryngeal carcinoma; EZH2; epithelial-mesenchymal transition; SFRP1; H3K27me3*

Laryngeal carcinoma (LGC) ranks the second most common head and neck neoplasm worldwide, with its progression initiating from the mucous layer to cartilage, cervical lymph nodes, and distant metastasis [1]. Since its symptoms at the early stage tend to be overlooked by most patients, such as breathing, swallowing, and voicing fatigues, most LGC cases (about 60%) are presented with the advanced stage at diagnosis [2]. In general, due to delayed detection and various limitations of existing treatments, the survival rate and prognosis of LGC patients have been little improved [3]. Epithelial-mesenchymal transition (EMT) is identified as a cellular program that provides epithelial cells with the property of mesenchymal stem cells [4]. The EMT activation of cancer cells leads to the invasion–metastasis cascade and resistance to therapeutic agents, thus promoting cancer development [5]. Against this backdrop, identifying molecular targets sensitive to the EMT of LGC cells is necessary to ensure the therapeutic efficacy of LGC treatment.

In the context of unchanged DNA sequencing, epigenetic modification is expected to hint at a promising strategy for LGC diagnosis and treatment through reversible alterations of gene expressions [6]. Enhancer of Zeste Homologue 2 (EZH2), one catalytic subunit of the polycomb repressive complex 2, exerts transcriptional suppressive functions through the introduction of trimethylation of lysine 27 on histone H3 (H3K27me3) [7]. Inherently, EZH2 is known to interact with EMT proteins, such as E-cadherin, N-cadherin, and vimentin, to facilitate the EMT program in lung adenocarcinoma, esophageal cancer, and glioblastoma [8–10]. Apart from its role in EMT regulation, EZH2 is found to have upregulation in LGC and encourage cell motility and autophagy [11, 12]. However, the mechanism of EZH2 in the EMT of LGC cells has not been fully understood.

As a histone methyltransferase, EZH2 degrades secreted frizzled-related protein 1 (SFRP1) via increasing H3K27me3 occupation on the SFRP1 promoter and further induces

Wnt/ $\beta$ -catenin signaling activation [13]. SFRP1, a member of the glycoprotein SFRP family, plays an epigenetic role in various cancer types, and its hypermethylation is associated with increased cancer risk [14]. SFRP1 was previously demonstrated to be epigenetically knocked down in LGC and SFRP1 overexpression could radically restrict the proliferation and colony formation of LGC cells [15]. In addition, SFRP1 is regarded to function as a Wnt (also dubbed as wingless and Int-1) modulator via binding to Wnt ligands in the cysteine-rich domain [16]. Wnt/ $\beta$ -catenin signaling considered as the canonical Wnt pathway is involved in multiple tumorigenic processes, such as cell survival, therapeutic resistance, and immune escape [17]. In particular, the  $\beta$ -catenin accumulation in the cytoplasm brings about its translocation in the nucleus, which further promotes the transcription of Wnt target oncogenes, thus leading to EMT [18]. The role of Wnt/ $\beta$ -catenin signaling in the proliferation, invasion, and migration of LGC cells has already been established [19]. However, the crosstalk of EZH2/SFRP1/Wnt in the EMT of LGC cells has not been discussed before and warrants profound investigation.

In light of the aforementioned data, we hypothesized that EZH2 regulates the EMT of LGC cells through interaction with the SFRP1-Wnt axis. In the current study, we analyzed the role of EZH2/SFRP1/Wnt in LGC through clinical sample detection and RNA interference, so as to provide a novel theoretical foundation for suppressing the EMT of LGC cells.

## Patients and methods

**Clinical sample acquisition.** Carcinoma and para-carcinoma tissues were resected from LGC patients ( $n = 70$ ) upon surgery. The diagnosis of LGC was confirmed by Jinling Hospital Affiliated with Nanjing University, and none patients received radiotherapy or chemotherapy prior to surgical treatment and were free from other immune diseases. The samples were confirmed by two experts of Jinling Hospital Affiliated with Nanjing University, frozen in liquid nitrogen immediately, and stored at  $-80^{\circ}\text{C}$ . The written consents were signed by all participants and the protocol was approved by the Ethics Committee of Jinling Hospital Affiliated with Nanjing University.

**Cell culture.** Human LGC cell lines (TU177, SNU46, M4E, and Tu686) and human nasopharyngeal epithelial

cells (HNPECs) NP69 were procured from the American Type Culture Collection (ATCC, Manassas, VA, USA) and cultured in Dulbecco's modified Eagle's medium/Ham's Nutrient Mixture F12 (DMEM/F12, Gibco, Life Technologies, Carlsbad, CA, USA) containing 10% (v/v) fetal bovine serum (FBS, Gibco, Life Technologies) and 1% (v/v) penicillin-streptomycin-glutamine (100 $\times$ , Gibco, Life Technologies) at  $37^{\circ}\text{C}$  with 5%  $\text{CO}_2$ .

**Cell transfection and treatment.** The siRNA sequences targeting EZH2 and SFRP1, SFRP1 overexpression pcDNA3.1 vector (oe-SFRP1), and their controls (empty plasmid was used for the control of overexpression vectors) were all provided by GenePharma (Shanghai, China). Cell transfection was carried out according to the instructions of Lipofectamine 2000 (Invitrogen, Carlsbad, CA, USA). The transfection effectiveness was detected after 24 h.

H3K27me3 agonist GSK-J4 (HY-15648B, MedChemExpress, USA) was employed for cell culture. Briefly, GSK-J4 was added into the culture medium at the final concentration of 10 nM, with dimethylsulfoxide (DMSO) as the blank control. Cells were cultured for 18 h before the subsequent experiments.

**Reverse transcription quantitative polymerase chain reaction (qRT-PCR).** RNA was extracted and reverse-transcribed using PureLink RNA microextraction kit (12193016, Thermo Fisher, Waltham, MA, USA) and RevertAid RT reverse transcription kit (K1691, Thermo Fisher). qRT-PCR was processed using SYBR<sup>®</sup> Premix Ex Taq<sup>™</sup> II (Perfect Real Time) kit (DRR081, Takara, Tokyo, Japan) and real-time quantification PCR analyzer (ABI 7500, ABI, Foster City, CA, USA), and the procedures followed the instructions of the kit. Primers of PCR were synthesized by Sangon Biotech (Shanghai, China) (primer sequences are shown in Table 1). The cycle threshold (Ct) value of each well was recorded and relative gene expressions were measured using the  $2^{-\Delta\Delta\text{Ct}}$  method with GAPDH as the internal reference.  $\Delta\Delta\text{Ct} = (\text{mean Ct value of target genes from the experiment group} - \text{mean Ct value of housekeeping genes from the experiment group}) - (\text{mean Ct value of target genes from the control group} - \text{mean Ct value from housekeeping genes of the control group})$  [20].

**Western blotting.** The cells or tissues were lysed with Radio Immunoprecipitation Assay buffer on ice. The concentration of protein contents was determined using the bicinchoninic acid kit. The protein fluid was separated using 12% sodium dodecyl sulfate-polyacrylamide gel electrophoresis and then transferred to polyvinylidene fluoride membranes. After blockage with 5% non-fat milk powder at room temperature for 2 h, membranes were washed with phosphate buffer saline (PBS) and PBS with Tween 20 (PBST), and cultured with the diluent of the primary anti-rabbit antibodies EZH2 (1:1000, 702492, Thermo Fisher),

**Table 1. qPCR primers.**

Gene	Forward Primer (5'-3')	Reverse Primer (5'-3')
EZH2	ACAGCGAAGGATACAGCCTGT	CAATGGTCAGCGGCTCCACAAGTA
SFRP1	ACGTGAGCTTCCAGTCGGACAT	CGTCAGCAAGTACTGGCTCTTCAC
GAPDH	CAGTCACTACTCAGCTGCCA	GAGGGTGCTCC GGTAG

**Table 2. ChIP-qPCR primers.**

Gene	Forward Primer (3'-5')	Reverse Primer (3'-5')
SFRP1	AGCTGTTGTGCTGATACCGTCCT	TGTTAGCCAGGCTGGTCTCGAAT

SFRP1 (1:1000, MA5-38193, Thermo Fisher), H3K27me3 (1:1000, MA5-11198, Thermo Fisher), E-cadherin (1:1000, 701134, Thermo Fisher), N-cadherin (1:1000, MA5-32088, Thermo Fisher),  $\beta$ -catenin (1:1000, MA5-29202, Thermo Fisher), c-Myc (1:1000, ab32072, Abcam), Cyclin D1 (1:100, ab16663, Abcam), and  $\beta$ -actin (1:1000, MA5-32479, Thermo Fisher) at 4°C overnight. After washing with PBS and PBST, the membranes were incubated with the secondary horseradish peroxidase-labeled goat anti-rabbit IgG (1:1000, 31460, Thermo Fisher) at room temperature for 1 h. The enhanced chemiluminescence working solution was used for image development and ImageJ software was used for semi-quantitative analysis of the bands with  $\beta$ -actin as the internal reference. The experiment of each group was conducted in triplicate.

**Cell viability detection.** Cell viability was assessed using the cell counting kit-8 (CCK-8) kit (HY-K0301, MedChem-Express, NJ, USA). Simply put,  $10^4$ /ml cell suspension was prepared and seeded into 96-well plates (100  $\mu$ l/well). After culture, 10  $\mu$ l CCK-8 solution was added to each well for 2 h, followed by detection of the absorbance at a wavelength of 450 nm. The experiment of each group was conducted in triplicate.

**Immunochemical staining.** Cells were fixed with 4% paraformaldehyde for 30 min and incubated with 0.5% Triton X-100 (Thermo Fisher) for 10 min. After 1 h of blockage with 10% goat serum and three washes with 1% serum blocking fluid, cells were incubated with the primary antibody anti-Vimentin (1:200, ab8978, Abcam) at 4°C overnight and then with the Alexa Fluor® 488-labeled secondary antibody IgG (1:200, ab150113, Abcam) at room temperature for 2 h. After that, cells were incubated with 4',6-diamidino-2-phenylindole in the dark for 5 min and photographed using a fluorescence microscope.

**Chromatin immunoprecipitation (ChIP)- qPCR.** ChIP assay was conducted using an EZ-Magna ChIP A kit (17-408, Sigma, St Louis, USA). Cells were fixed with 1% methanol at 37°C for 10 min, added with glycine at the final concentration of 0.125 M, and left at room temperature for 5 min. The fixed cells were re-suspended with the mixture of cell lysis buffer (10 mmol/l Tris-HCl, pH 7.5, 10 mmol/l NaCl, 0.5% NP-40) and the protease inhibitor on ice for 10 min. After washing with cold PBS, the lysis solution was re-suspended using the sonication buffer and chromatin was ultrasonically sheared into 500–2000 bp fragments. Then, the Protein A Agarose/Salmon Sperm DNA was added to the supernatant diluted with ChIP buffer. After centrifugation, the supernatant was collected and incubated with Anti-Histone H3K27me3 (ab6002, Abcam, Cambridge, MA, USA) or IgG overnight for immunoprecipitation, followed by quantitative analysis using qRT-PCR. The enrichment level of H3K27me3 in the SFRP1 promoter was calculated with IgG as the control. The primer sequences of ChIP-qPCR are shown in Table 2. The experiment of each group was conducted in triplicate.

**Statistical analysis.** The data analysis and graphing were processed using the SPSS21.0 statistical software (IBM Corp, Armonk, NY, USA) and GraphPad Prism 8.0 software (GraphPad Software Inc., San Diego, CA, USA). All data were represented as mean  $\pm$  standard deviation (SD) and conformed to normal distribution and homogeneity of variance. The t-test was employed for pairwise comparisons, one-way or two-way analysis of variance (ANOVA) was employed for multi-group comparisons, Tukey's multiple comparison test was employed for the post-test, and Pearson Correlation Coefficient was employed for correlation analysis. p-value was obtained from two-sided tests. A value of  $p < 0.05$  indicated statistical significance.

## Results

EZH2 was highly expressed in LGC tissues and cell lines. To analyze the expression pattern of EZH2 in LGC cells, we detected the mRNA level of EZH2 in tissues and cell lines via qRT-PCR. Compared with para-carcinoma tissues, the mRNA level of EZH2 was increased in carcinoma tissues ( $p < 0.05$ , Figure 1A). Compared with HNPECs (NP69), the mRNA level of EZH2 was increased in LGC cell lines ( $p < 0.05$ , Figure 1A). Meanwhile, we detected the protein level of EZH2 in tissues and cells via western blotting, which indicated that the protein level of EZH2 was elevated in LGC tissues and cells compared with carcinoma tissues and HNPECs ( $p < 0.05$ , Figure 1B). Altogether, these findings elucidated that EZH2 was highly expressed in LGC tissues and cells.

EZH2 downregulation inhibited the EMT of LGC cells. To analyze the role of EZH2 in the EMT of LGC cells, we selected TU177 and Tu686 cells with comparatively higher expression of EZH2 for the subsequent experiments. We designed two strands of si-RNA and transfected them into TU177 and Tu686 cells to downregulate EZH2 expression ( $p < 0.05$ , Figure 2A). si-EZH2-1 with a higher transfection efficiency was utilized for the subsequent experiments. CCK-8 assay was performed to assess cell viability, which indicated that cell viability was declined in the si-EZH2-1 group compared with the si-NC group ( $p < 0.05$ , Figure 2B). Then, western blotting and immunofluorescence assays were performed to detect protein expressions of EMT markers (E-cadherin, N-cadherin, and Vimentin), which indicated that E-cadherin expression was increased while N-cadherin was decreased ( $p < 0.05$ , Figure 2C), and fluorescence intensity of Vimentin was weakened (Figure 2D) in si-EZH2-1-transfected cells. Altogether, these findings elucidated that EZH2 downregulation inhibited the EMT of LGC cells.

**EZH2 upregulated H3K27me3 in the SFRP1 promoter to inhibit SFRP1.** To further analyze the molecular mechanism of EZH2 in LGC cells, we detected the H3K27me3 level via western blotting. Compared with the si-NC group, the protein level of H3K27me3 was markedly decreased in the si-EZH2-1 group ( $p < 0.05$ , Figure 3A). Then, the ChIP-qPCR assay showed that compared with the si-NC group,

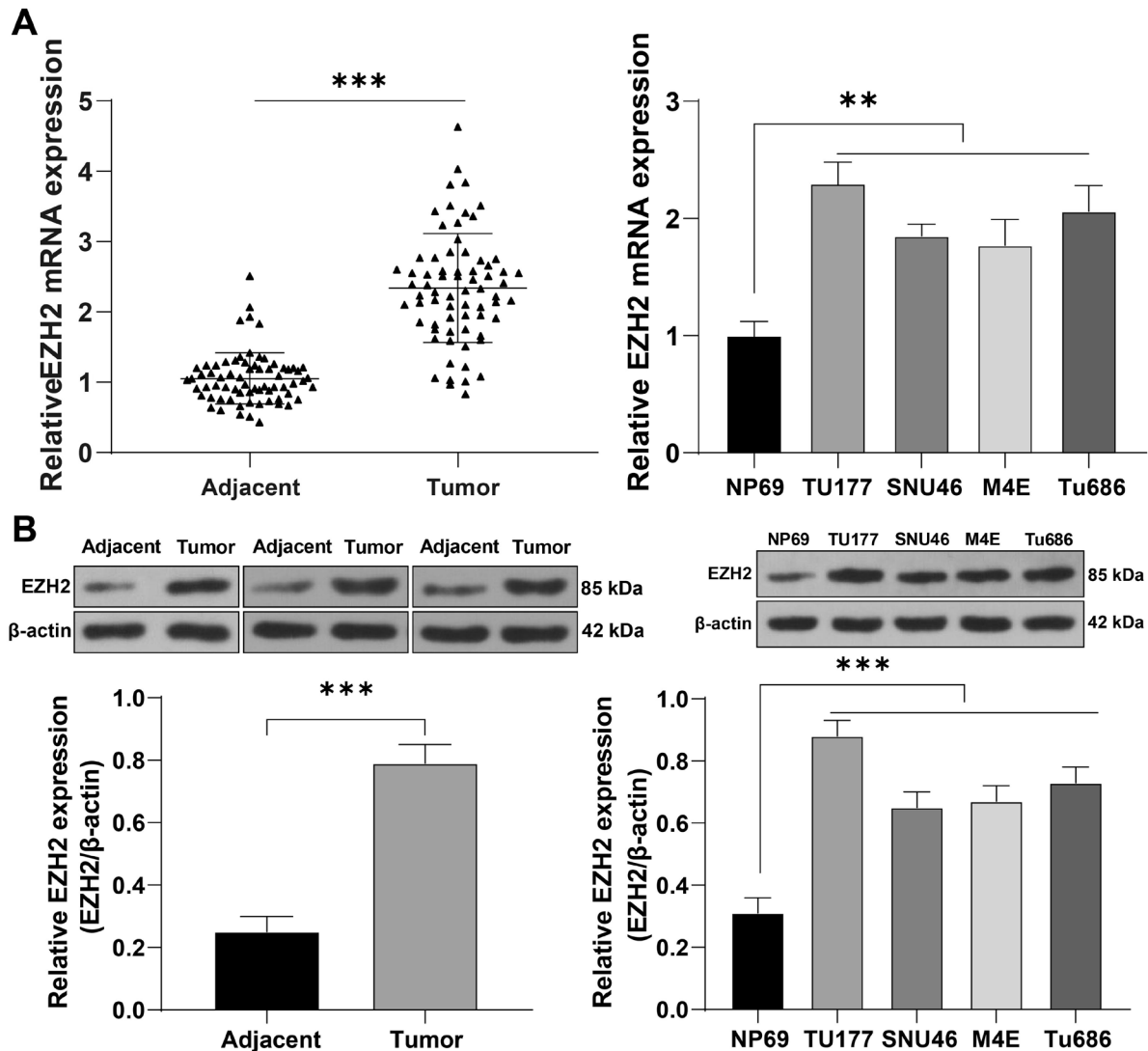


Figure 1. EZH2 was highly expressed in LGC tissues and cell lines. A) mRNA level of EZH2 in tissues ( $n = 70$ ) and cell lines (TU177, SNU46, M4E, Tu686, and NP69) was detected via qRT-PCR; B) Protein level of EZH2 in tissues ( $n = 70$ ) and cell lines (TU177, SNU46, M4E, Tu686, and NP69) was detected via western blotting. Cell experiments were performed 3 times independently, and data are represented as mean  $\pm$  SD, \*\*\* $p < 0.001$ , \*\* $p < 0.01$ . Data in figure A (left) were analyzed using the paired t-test, data in figure B (left) were analyzed using the unpaired t-test, and data in figure A (right) and figure B (right) were analyzed using one-way ANOVA, followed by Tukey's multiple comparison test.

the enrichment level of H3K27me3 in the SFRP1 promoter was markedly reduced in the si-EZH2-1 group ( $p < 0.05$ , Figure 3B). Furthermore, we detected SFRP1 expression via qRT-PCR and western blotting, which showed that SFRP1 expression was higher in the si-EZH2-1 group compared with the si-NC group ( $p < 0.05$ , Figure 3C). Altogether, these findings elucidated that EZH2 upregulated H3K27me3 in the SFRP1 promoter to inhibit SFRP1 expression.

H3K27me3 upregulation partly reversed the inhibition of silencing EZH2 in the EMT of LGC cells. Next, we validated the above mechanism through a rescue experiment. First, GSK-J4 hydrochloride (H3K27me3 agonist)

was used to upregulate the H3K27me3 level in TU177 cells ( $p < 0.05$ , Figure 4A), followed by a collaborative experiment with si-EZH2-1 which has better transfection effectiveness. We detected the SFRP1 expression in TU177 cells via western blotting and the results revealed that SFRP1 expression was lower in the si-EZH2-1+GSK-J4 group compared with the si-EZH2-1 and si-EZH2-1+DMSO groups ( $p < 0.05$ , Figure 4B). Subsequently, CCK-8 results showed that cell viability in the si-EZH2-1+GSK-J4 group was augmented compared with the si-EZH2-1 and si-EZH2-1+DMSO groups ( $p < 0.05$ , Figure 4C), and western blotting and immunofluorescence assays revealed that E-cadherin expression

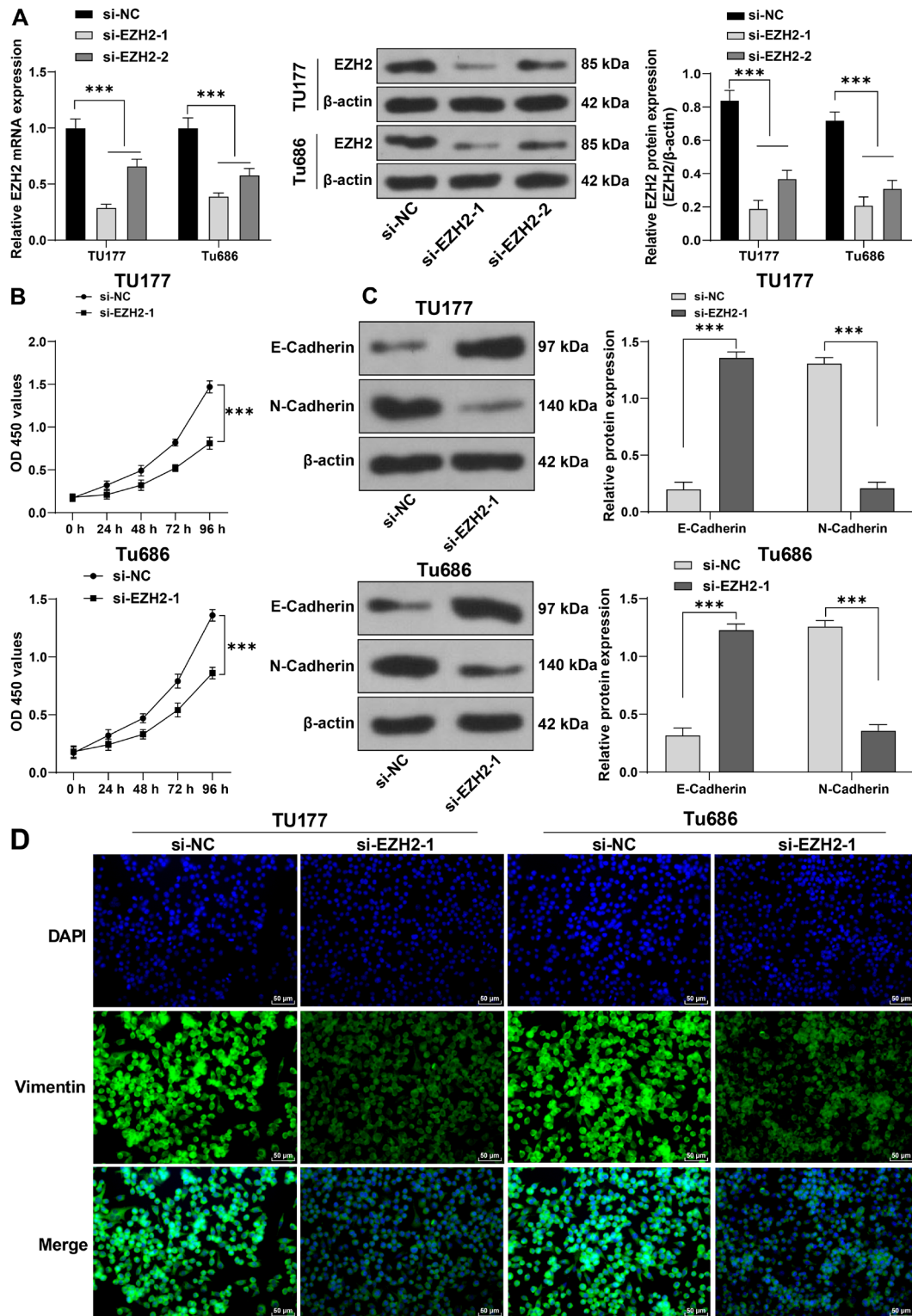
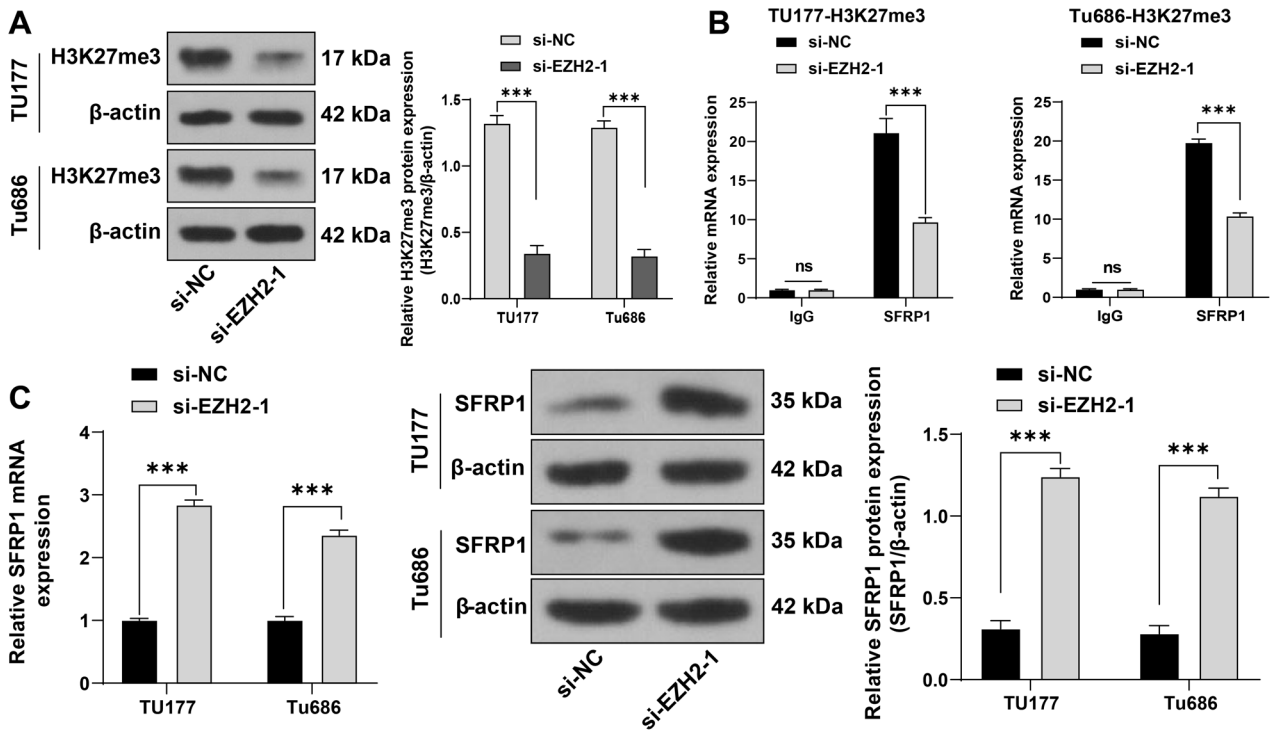


Figure 2. EZH2 downregulation inhibited the EMT of LGC cells. TU177 and Tu686 cells were transfected with si-EZH2-1 and si-EZH2-2, with si-NC as the control. A) Transfection effectiveness of si-EZH2-1 and si-EZH2-2 was determined via qRT-PCR and western blotting; B) Cell viability was assessed via CCK-8 assay; C) Protein expressions of E-cadherin and N-cadherin were detected via western blotting; D) Vimentin expression was detected via immunofluorescence assay. Cell experiments were performed 3 times independently, and data are represented as mean  $\pm$  SD, \*\*\* $p$ <0.001. Data in figures A-C were analyzed using two-way ANOVA, followed by Tukey's multiple comparison test.



**Figure 3.** EZH2 upregulated H3K27me3 in the SFRP1 promoter to inhibit SFRP1. A) Protein level of H3K27me3 was detected via western blotting; B) Enrichment level of H3K27me3 in the SFRP1 promoter was measured via ChIP-qPCR assay; C) SFRP1 expression was detected via qRT-PCR and western blotting. Cell experiments were performed 3 times independently, and data are represented as mean ± SD, \*\*\*p<0.001, ns: p>0.05. Data in figures A–C were analyzed using two-way ANOVA, followed by Tukey’s multiple comparison test.

was decreased, while N-cadherin expression was increased (p<0.05, Figure 4D), and fluorescence intensity of Vimentin was enhanced (Figure 4E) in the si-EZH2-1 + GSK-J4 group when compared with the si-EZH2-1 and si-EZH2-1 + DMSO groups. Altogether, these findings elucidated that H3K27me3 upregulation partly reversed the inhibition of silencing EZH2 in the EMT of LGC cells.

SFRP1 upregulation inhibited the Wnt signaling activation. To analyze the downstream mechanism of SFRP1 in LGC cells, we overexpressed SFRP1 in TU177 and Tu686 cells using pcDNA3.1-SFRP1 (p<0.05, Figure 5A). Then, the protein levels of SFRP1, β-catenin, c-Myc, and Cyclin D1 were detected via western blotting, which showed that compared with the oe-NC group, the protein level of SFRP1 was increased while the protein levels of β-catenin, c-Myc, and Cyclin D1 were decreased in the oe-SFRP1 group (p<0.05, Figures 5B, 5C). Altogether, these findings elucidated that SFRP1 upregulation inhibited the Wnt signaling activation.

SFRP1 downregulation reversed the inhibition of silencing EZH2 in EMT of LGC cells via activating the Wnt signaling pathway. Next, we validated the above mechanism through a rescue experiment. Two strands of si-RNA were designed and transfected into TU177 cells. The detection of qRT-PCR

showed that SFRP1 mRNA expression was markedly lowered in the si-SFRP1-1 and siSFRP1-2 groups (p<0.05, Figure 6A). si-SFRP1-2 with better transfection effectiveness was combined with si-EZH2-1 for the next collaborative experiment. The protein level of β-catenin was detected via western blotting, which showed that the protein levels of β-catenin, c-Myc, and Cyclin D1 in the si-EZH2-1+siSFRP1-2 groups were higher than that in the si-EZH2-1 and si-EZH2-1+si-NC groups (p<0.05, Figure 6B). Subsequently, the CCK-8 assay showed that cell viability in the si-EZH2-1+siSFRP1-2 groups was elevated compared with the si-EZH2-1 and si-EZH2-1+si-NC groups (p<0.05, Figure 6C). Moreover, western blotting showed that E-cadherin expression was decreased while N-cadherin expression was increased in the si-EZH2-1+siSFRP1-2 groups compared with the si-EZH2-1 and si-EZH2-1+si-NC groups (p<0.05, Figure 6D). Altogether, these findings elucidated that SFRP1 downregulation reversed the inhibition of silencing EZH2 in the EMT of LGC cells via activating the Wnt signaling pathway.

**Discussion**

Histone methylation as a critical component of the epigenetic modification system has been given great interest in the

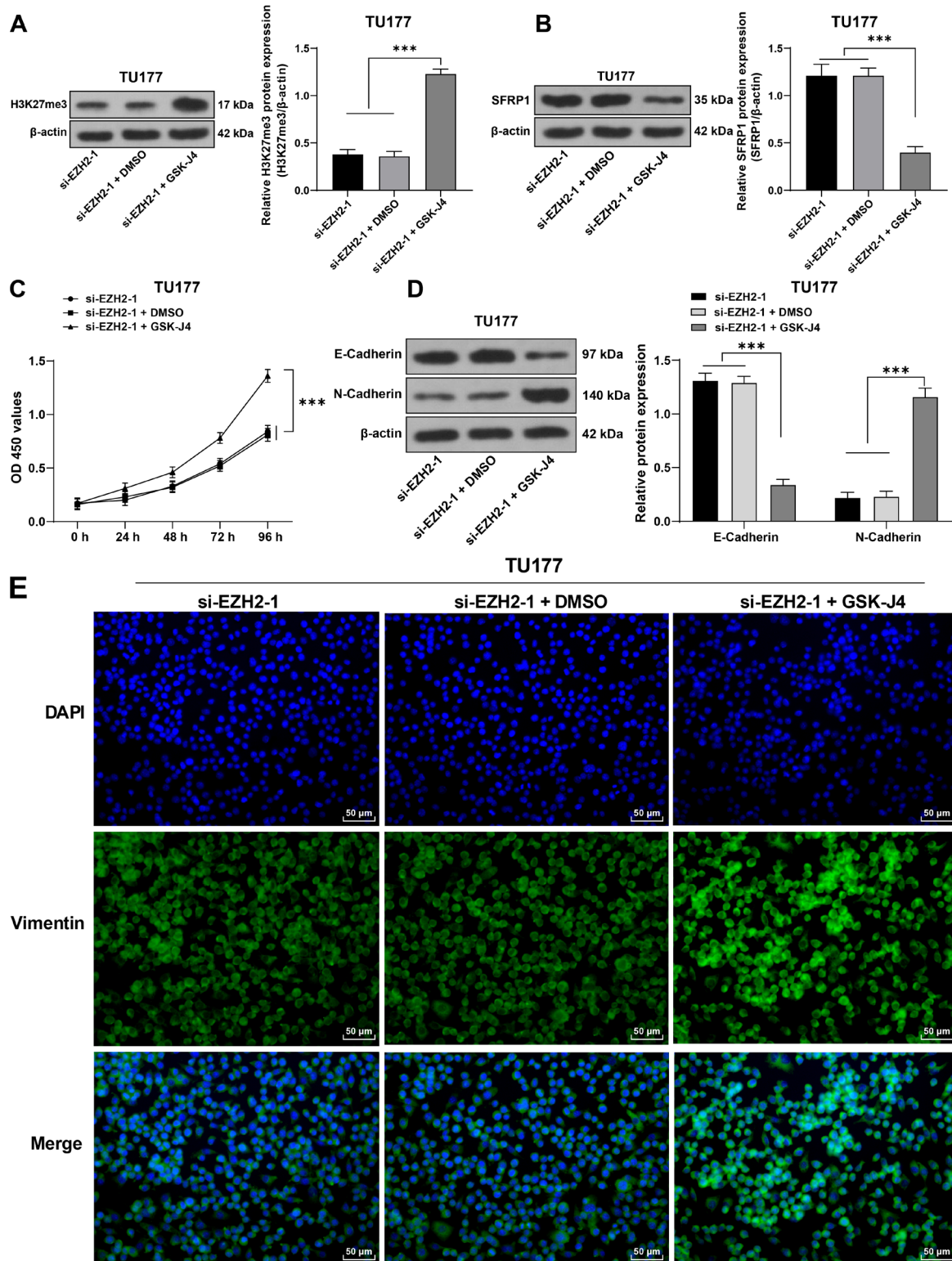
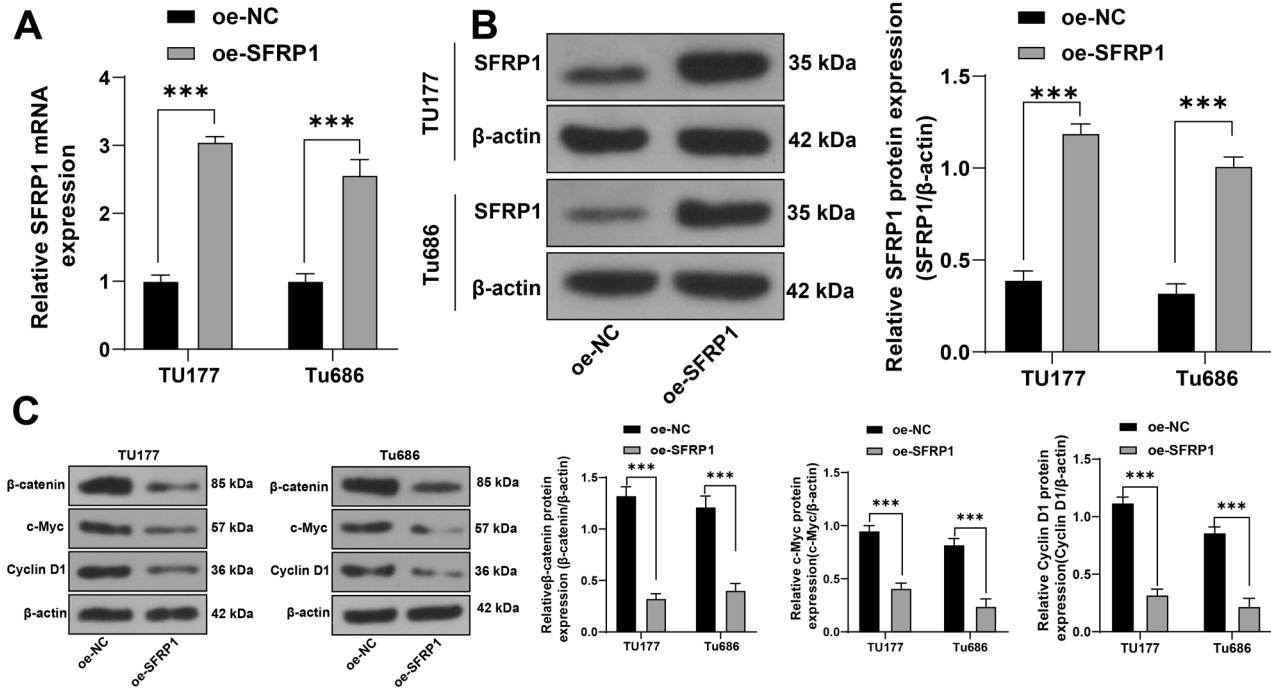


Figure 4. H3K27me3 upregulation partly reversed the inhibition of silencing EZH2 in the EMT of LGC cells. A) H3K27me3 level in GSK-J4-treated TU177 cells was detected via western blotting; B) Protein level of SFRP1 was detected via western blotting; C) Cell viability was assessed via CCK-8 assay; D) Protein levels of E-cadherin and N-cadherin were detected via western blotting; E) Vimentin expression was detected via immunofluorescence assay. Cell experiments were performed 3 times independently, and data are represented as mean  $\pm$  SD, \*\*\* $p$ <0.001. Data in figures A and B were analyzed using one-way ANOVA, and data in figures C and D were analyzed using two-way ANOVA, followed by Tukey's multiple comparison test.



**Figure 5.** SFRP1 upregulation inhibited the Wnt signaling activation. TU177 and Tu686 cells were transfected with pcDNA3.1-SFRP1 (oe-SFRP1), with pcDNA-3.1 (oe-NC) as the control. A) Transfection effectiveness of oe-SFRP1 was detected via qRT-PCR; B, C) Protein level of oe-SFRP1,  $\beta$ -catenin, c-Myc, and Cyclin D1 was detected via western blotting. Cell experiments were performed 3 times independently, and data are represented as mean  $\pm$  SD, \*\*\* $p$ <0.001. Data in figures A–C were analyzed using two-way ANOVA, followed by Tukey's multiple comparison test.

investigation in oncology to offer more molecular targets in the clinic [21]. EZH2 as a histone methyltransferase participates in the regulation of cancer cell growth, metastasis, metabolism, resistance to agents, and cancer immunity [22]. In the present study, our findings highlighted that EZH2 upregulates H3K27me3 in the SFRP1 promoter to inhibit SFRP1 expression and activate the Wnt/ $\beta$ -catenin signaling, thus facilitating the EMT of LGC cells.

Prior studies have demonstrated that EZH2 is ectopically expressed in LGC and EZH2 overexpression potentiates LGC cell proliferation and autophagy [11, 12]. In regard to clinical significance, increased EZH2 could predict the prognosis of LGC patients [23]. Accordingly, both increased mRNA and protein expressions of EZH2 were found in LGC tissues and cell lines (TU177, SNU46, M4E, Tu686, and NP69). To explore the role of EZH2 in LGC cells, EZH2 expression was downregulated in TU177 and Tu686 cells via si-RNA, and we observed that EZH2 downregulation reduced cell viability. EMT is a crucial promoter of tumorigenesis, accompanied by increases in N-cadherin and Vimentin and a decrease in E-cadherin [24]. Our experiment showed that E-cadherin and Vimentin were increased while N-cadherin diminished in TU177 and Tu686 cells as a response to EZH2 downregulation, indicating that EZH2 downregulation inhibited the EMT of LGC. In consistence with our results, silencing EZH2 also repels the EMT in esophageal, lung, ovarian, and breast

cancers [10, 25–27]. Taken together, we demonstrated that EZH2 downregulation inhibits the EMT of LGC cells.

EZH2 is known to play a silencing role in a spectrum of downstream cancer-related genes, thus affecting cancer development [7]. Notably, EZH2 recruited H3K27me3 to the SFRP1 promoter to silence SFRP1 expression, consequently increasing the Wnt/ $\beta$ -catenin signaling in osteoarthritis [13]. Our subsequent experiments showed that the H3K27me3 level was decreased in LGC cells and the enrichment level of H3K27me3 in the SFRP1 promoter was reduced upon EZH2 downregulation, indicating that EZH2 upregulated H3K27me3 in the SFRP1 promoter to inhibit SFRP1 expression in LGC cells. On top of that, the H3K27me3 level was upregulated using an agonist GSK-J4 hydrochloride in TU177 cells and combined with the treatment of EZH2 downregulation for rescue experiments. We observed that H3K27me3 upregulation reversed the inhibition of silencing EZH2 in the EMT of LGC cells. Similarly, recruitment of H3K27me3 is associated with cancer cell phenotype in melanoma, small cell lung cancer, and prostate cancer [28–30]. Collectively, we demonstrated that EZH2 plays a driving role in the EMT of LGC cells via upregulating H3K27me3 in the SFRP1 promoter.

Loss of SFRP1 expression is often attributed to promoter hypermethylation and epigenetic silencing of SFRP1 gives rise to cancer initiation and development [14]. More impor-

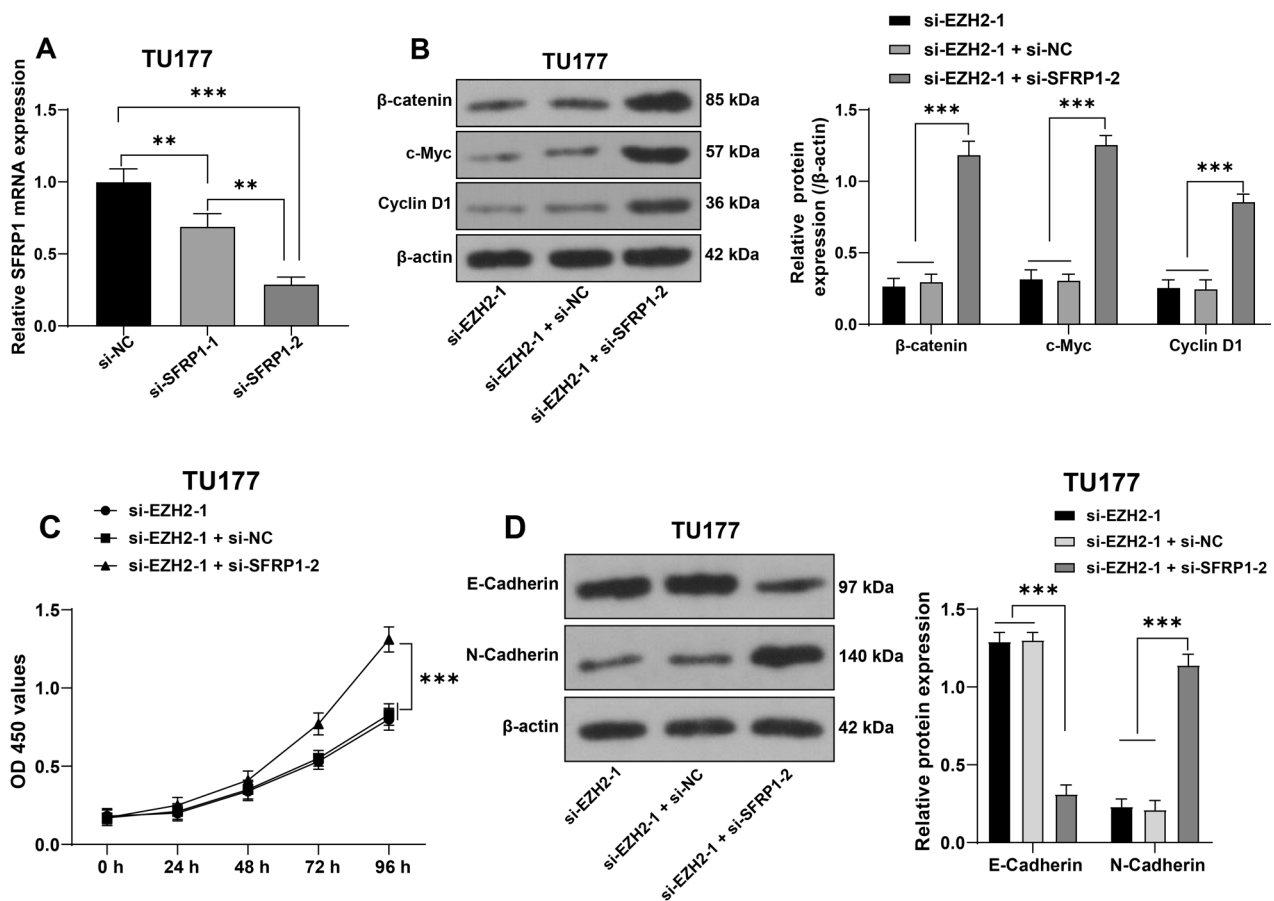


**Figure 6.** SFRP1 downregulation reversed the inhibition of silencing EZH2 in the EMT of LGC cells via activating the Wnt signaling pathway. TU177 cells were transfected with si-SFRP1-1 and si-SFRP1-2, with si-NC as the control. A) Transfection effectiveness of si-SFRP1-1 and si-SFRP1-2 was determined via qRT-PCR. si-SFRP1-2 and si-EZH2-1 with better transfection effectiveness were used for the collaborative experiment. B) Protein level of  $\beta$ -catenin, c-Myc, and Cyclin D1 was detected via western blotting; C) Cell viability was assessed via CCK-8 assay; D) Protein levels of E-cadherin and N-cadherin were detected via western blotting. Cell experiments were performed 3 times independently, and data are represented as mean  $\pm$  SD, \*\*\* $p$ <0.001. Data in figure A were analyzed using one-way ANOVA, and data in figures B, C and D were analyzed using two-way ANOVA, followed by Tukey's multiple comparison test.

tantly, overexpressed SFRP1 is found to retard LGC progression and increase cell drug sensitivity [15]. In terms of its downstream mechanism, SFRP1 is reported to serve as an inhibitor of the Wnt/ $\beta$ -catenin signaling which is one of the well-established EMT-related signaling [31], and  $\beta$ -catenin, c-Myc, and Cyclin D1 are the pivotal proteins to activate the canonical Wnt pathway [32]. Accordingly, it was observed that the protein level of  $\beta$ -catenin along with c-Myc and Cyclin D1 was reduced upon SFRP1 overexpression, confirming that SFRP1 overexpression inhibited the Wnt pathway activation. In addition, we silenced SFRP1 and EZH2 simultaneously in TU177 cells and observed that SFRP1 downregulation induced the EMT of LGC cells by activating the Wnt pathway. Consistently, SFRP1 potentiates the Wnt-induced EMT phenotype in non-small cell lung cancer, colorectal cancer, hepatocellular carcinoma, and breast cancer [33–36]. Yet, the epigenetic network of EZH2/

SFRP1/Wnt in LGC has not been studied before, which highlights the novelty of our study. Overall, we initially demonstrated that SFRP1 downregulation reversed the inhibition of silencing EZH2 in the EMT of LGC cells via activating the Wnt pathway.

To conclude, our data identified that EZH2 functioning as a histone methyltransferase plays a driving role in the EMT of LGC cells via manipulation of SFRP1/Wnt signaling, which may provide a brand-new tailored strategy for LGC clinical management from the perspective of epigenetic modification. However, our study failed to validate the role of EZH2/SFRP1/Wnt in animals. In the next step, we will further confirm the role of EZH2 through animal models and collect more clinical samples to explore other molecular mechanisms in the EMT of LGC cells, and whether EZH2-SFRP1-Wnt signal-mediated EMT affects LGC cell migration and invasion so as to improve the integrity of our study.

Acknowledgments: This work was supported by China Postdoctoral Science Foundation [grant numbers 2018T111165, 2017M623435]; and China Jiangsu Planned Projects for Jiangsu Provincial Medical Talent [grant number QNRC2016917].

## References

- [1] QU J, ZHANG M, WEI W, YANG Y. [Progress in CT and MRI of preoperative T staging of laryngeal carcinoma]. *Lin Chung Er Bi Yan Hou Tou Jing Wai Ke Za Zhi* 2020; 34: 470–474. <https://doi.org/10.13201/j.issn.2096-7993.2020.05.022>
- [2] STEUER CE, EL-DEIRY M, PARKS JR, HIGGINS KA, SABA NF. An update on larynx cancer. *CA Cancer J Clin* 2017; 67: 31–50. <https://doi.org/10.3322/caac.21386>
- [3] OBID R, REDLICH M, TOMEH C. The Treatment of Laryngeal Cancer. *Oral Maxillofac Surg Clin North Am* 2019; 31: 1–11. <https://doi.org/10.1016/j.coms.2018.09.001>
- [4] BABAEI G, AZIZ SG, JAGHI NZZ. EMT, cancer stem cells and autophagy; The three main axes of metastasis. *Biomed Pharmacother* 2021; 133: 110909. <https://doi.org/10.1016/j.biopha.2020.110909>
- [5] DONGRE A, WEINBERG RA. New insights into the mechanisms of epithelial-mesenchymal transition and implications for cancer. *Nat Rev Mol Cell Biol* 2019; 20: 69–84. <https://doi.org/10.1038/s41580-018-0080-4>
- [6] MENG WX, WANG BS. [Epigenetic regulations in laryngeal squamous cell carcinoma]. *Lin Chung Er Bi Yan Hou Tou Jing Wai Ke Za Zhi* 2018; 32: 1958–1762. <https://doi.org/10.13201/j.issn.1001-1781.2018.22.019>
- [7] LU H, LI G, ZHOU C, JIN W, QIAN X et al. Regulation and role of post-translational modifications of enhancer of zeste homologue 2 in cancer development. *Am J Cancer Res* 2016; 6: 2737–2754.
- [8] STAZI G, TAGLIERI L, NICOLAI A, ROMANELLI A, FIORAVANTI R et al. Dissecting the role of novel EZH2 inhibitors in primary glioblastoma cell cultures: effects on proliferation, epithelial-mesenchymal transition, migration, and on the pro-inflammatory phenotype. *Clin Epigenetics* 2019; 11: 173. <https://doi.org/10.1186/s13148-019-0763-5>
- [9] MATSUBARA T, TOYOKAWA G, TAKADA K, KINOSHITA F, KOZUMA Y et al. The association and prognostic impact of enhancer of zeste homologue 2 expression and epithelial-mesenchymal transition in resected lung adenocarcinoma. *PLoS One* 2019; 14: e0215103. <https://doi.org/10.1371/journal.pone.0215103>
- [10] ZHANG S, LIAO W, WU Q, HUANG X, PAN Z et al. LINC00152 upregulates ZEB1 expression and enhances epithelial-mesenchymal transition and oxaliplatin resistance in esophageal cancer by interacting with EZH2. *Cancer Cell Int* 2020; 20: 569. <https://doi.org/10.1186/s12935-020-01620-1>
- [11] LIAN R, MA H, WU Z, ZHANG G, JIAO L et al. EZH2 promotes cell proliferation by regulating the expression of RUNX3 in laryngeal carcinoma. *Mol Cell Biochem* 2018; 439: 35–43. <https://doi.org/10.1007/s11010-017-3133-7>
- [12] CHEN L, JIA J, ZANG Y, LI J, WAN B. MicroRNA-101 regulates autophagy, proliferation and apoptosis via targeting EZH2 in laryngeal squamous cell carcinoma. *Neoplasma* 2019; 66: 507–515. [https://doi.org/10.4149/neo\\_2018\\_180811N611](https://doi.org/10.4149/neo_2018_180811N611)
- [13] CHEN L, WU Y, WU Y, WANG Y, SUN L et al. The inhibition of EZH2 ameliorates osteoarthritis development through the Wnt/beta-catenin pathway. *Sci Rep* 2016; 6: 29176. <https://doi.org/10.1038/srep29176>
- [14] BAHARUDIN R, TIENG FYE, LEE LH, AB MUTALIB NS. Epigenetics of SFRP1: The Dual Roles in Human Cancers. *Cancers (Basel)* 2020; 12: 445. <https://doi.org/10.3390/cancers12020445>
- [15] WU KM, LI ZQ, YI WZ, WU MH, JIANG MJ et al. Restoration of secreted frizzled-related protein 1 suppresses growth and increases cisplatin sensitivity in laryngeal carcinoma cells by downregulating NHE1. *Int J Clin Exp Pathol* 2017; 10: 8334–8343.
- [16] BOUDIN E, FIJALKOWSKI I, PITERS E, VAN HUL W. The role of extracellular modulators of canonical Wnt signaling in bone metabolism and diseases. *Semin Arthritis Rheum* 2013; 43: 220–240. <https://doi.org/10.1016/j.semarthrit.2013.01.004>
- [17] MARTIN-OROZCO E, SANCHEZ-FERNANDEZ A, ORTIZ-PARRA I, AYALA-SAN NICOLAS M. WNT Signaling in Tumors: The Way to Evade Drugs and Immunity. *Front Immunol* 2019; 10: 2854. <https://doi.org/10.3389/fimmu.2019.02854>
- [18] LEI Y, CHEN L, ZHANG G, SHAN A, YE C et al. MicroRNAs target the Wnt/betacatenin signaling pathway to regulate epithelialmesenchymal transition in cancer (Review). *Oncol Rep* 2020; 44: 1299–1313. <https://doi.org/10.3892/or.2020.7703>
- [19] SUN S, GONG C, YUAN K. LncRNA UCA1 promotes cell proliferation, invasion and migration of laryngeal squamous cell carcinoma cells by activating Wnt/beta-catenin signaling pathway. *Exp Ther Med* 2019; 17: 1182–1189. <https://doi.org/10.3892/etm.2018.7097>
- [20] LIVAK KJ, SCHMITTGEN TD. Analysis of relative gene expression data using real-time quantitative PCR and the 2(-Delta Delta C(T)) Method. *Methods* 2001; 25: 402–408. <https://doi.org/10.1006/meth.2001.1262>
- [21] MCCABE MT, MOHAMMAD HP, BARBASH O, KRUGER RG. Targeting Histone Methylation in Cancer. *Cancer J* 2017; 23: 292–301. <https://doi.org/10.1097/PPO.000000000000283>
- [22] DUAN R, DU W, GUO W. EZH2: a novel target for cancer treatment. *J Hematol Oncol* 2020; 13: 104. <https://doi.org/10.1186/s13045-020-00937-8>
- [23] ZHANG MJ, CHEN DS, LI H, LIU WW, HAN GY et al. Clinical significance of USP7 and EZH2 in predicting prognosis of laryngeal squamous cell carcinoma and their possible functional mechanism. *Int J Clin Exp Pathol* 2019; 12: 2184–2194.
- [24] LOH CY, CHAI JY, TANG TF, WONG WF, SETHI G et al. The E-Cadherin and N-Cadherin Switch in Epithelial-to-Mesenchymal Transition: Signaling, Therapeutic Implications, and Challenges. *Cells* 2019; 8: 1118. <https://doi.org/10.3390/cells8101118>

- [25] PATTANAYAK B, GARRIDO-CANO I, ADAM-ARTIGUES A, TORMO E, PINEDA B et al. MicroRNA-33b Suppresses Epithelial-Mesenchymal Transition Repressing the MYC-EZH2 Pathway in HER2+ Breast Carcinoma. *Front Oncol* 2020; 10: 1661. <https://doi.org/10.3389/fonc.2020.01661>
- [26] CARDENAS H, ZHAO J, VIETH E, NEPHEW KP, MATTEI D. EZH2 inhibition promotes epithelial-to-mesenchymal transition in ovarian cancer cells. *Oncotarget* 2016; 7: 84453–84467. <https://doi.org/10.18632/oncotarget.11497>
- [27] ROCHE J, GEMMILL RM, DRABKIN HA. Epigenetic Regulation of the Epithelial to Mesenchymal Transition in Lung Cancer. *Cancers (Basel)* 2017; 9: 72. <https://doi.org/10.3390/cancers9070072>
- [28] NGOLLO M, LEBERT A, DAURES M, JUDES G, RIFAI K et al. Global analysis of H3K27me3 as an epigenetic marker in prostate cancer progression. *BMC Cancer* 2017; 17: 261. <https://doi.org/10.1186/s12885-017-3256-y>
- [29] FANG S, SHEN Y, CHEN B, WU Y, JIA L et al. H3K27me3 induces multidrug resistance in small cell lung cancer by affecting HOXA1 DNA methylation via regulation of the lncRNA HOTAIR. *Ann Transl Med* 2018; 6: 440. <https://doi.org/10.21037/atm.2018.10.21>
- [30] HOFFMANN F, NIEBEL D, AYMANS P, FERRINGSCHMITT S, DIETRICH D et al. H3K27me3 and EZH2 expression in melanoma: relevance for melanoma progression and response to immune checkpoint blockade. *Clin Epigenetics* 2020; 12: 24. <https://doi.org/10.1186/s13148-020-0818-7>
- [31] ZHANG H, SUN D, QIU J, YAO L. SFRP1 inhibited the epithelial ovarian cancer through inhibiting Wnt/beta-catenin signaling. *Acta Biochim Pol* 2019; 66: 393–400. [https://doi.org/10.18388/abp.2019\\_2757](https://doi.org/10.18388/abp.2019_2757)
- [32] ZHANG Y, WANG X. Targeting the Wnt/beta-catenin signaling pathway in cancer. *J Hematol Oncol* 2020; 13: 165. <https://doi.org/10.1186/s13045-020-00990-3>
- [33] ZHANG D, LIU X, LI Y, SUN L, LIU SS et al. LINC01189-miR-586-ZEB1 feedback loop regulates breast cancer progression through Wnt/beta-catenin signaling pathway. *Mol Ther Nucleic Acids* 2021; 25: 455–467. <https://doi.org/10.1016/j.omtn.2021.06.007>
- [34] MOSA MH, MICHELS BE, MENCHE C, NICOLAS AM, DARVISHI T et al. A Wnt-Induced Phenotypic Switch in Cancer-Associated Fibroblasts Inhibits EMT in Colorectal Cancer. *Cancer Res* 2020; 80: 5569–5582. <https://doi.org/10.1158/0008-5472.CAN-20-0263>
- [35] LIN XH, LIU HH, HSU SJ, ZHANG R, CHEN J et al. Nor-epinephrine-stimulated HSCs secrete sFRP1 to promote HCC progression following chronic stress via augmentation of a Wnt16B/beta-catenin positive feedback loop. *J Exp Clin Cancer Res* 2020; 39: 64. <https://doi.org/10.1186/s13046-020-01568-0>
- [36] LI X, LV F, LI F, DU M, LIANG Y et al. LINC01089 Inhibits Tumorigenesis and Epithelial-Mesenchymal Transition of Non-small Cell Lung Cancer via the miR-27a/SFRP1/Wnt/beta-catenin Axis. *Front Oncol* 2020; 10: 532581. <https://doi.org/10.3389/fonc.2020.532581>